Proceeding of the 2004 American Control Conference
Boston, Massachusetts June 30 - July 2, 2004

Adaptive observer for traffic density estimation

Luis Alvarez-Icaza, Laura Munoz, Xiaotian Sun and Roberto Horowitz

Abstract— A traffic density scheme to be used for real-time on-ramp metering control to freeways is proposed. The scheme can be used in two situations: a) When there are no traffic flow sensors appropriately located and b) When available sensors are faulty. It is assumed that some traffic flow and velocity measurements are available in the vicinity of the place where an on-ramp is located. Based on this information, a non-linear adaptive observer for vehicle density is designed that also estimates the mixing factors that define the traffic flow characteristics: free or congested. The design is based on Lyapunov techniques that take advantage of the structure of the conservation of vehicles model.

I. Introduction

Increasing the efficiency in freeways is a high priority task in many cities across the world. This has to be done in a context where, simultaneously, there is a growing demand for ground transportation and there exists severe environmental and real state limitations for the construction of new infrastructure. The traditional approach to solve the traffic congestion problems has shown to be insufficient, so new technologies are being deployed in an attempt to solve them [1], [2]. Adaptive cruise control, advanced traction and braking control, driver alert systems, variable signal systems and real-time on ramp metering control are among these new technologies.

The goal of on-ramp control techniques is to dose drivers access to freeway trying to avoid worsening traffic congestion. There is a price to pay for the drivers in terms of waiting time in the on-ramp. However, this waiting time is easily compensated with the decrease in the travel time of a trip on an uncongested freeway.

To implant these on-ramp control techniques in freeways, traffic information is required. Some of this information is already available in many cities traffic management control centers that handle flow, occupancy, velocity and vehicle density for a number of points in the freeways network. In most of the cases, however, this information is not used for real-time control.

There are already some closed loop control techniques whose purpose is to alleviate freeway congestion[3], [4], [5]. These control techniques require measurements of density or occupancy. In many cases, however, these measurements are not obtained in places close enough to the on-ramp or the available sensors are faulty. These two problems make it necessary to design traffic estimation schemes to recover the missing information.

In this paper an estimation scheme for vehicle density in the middle section of a stretch of freeway is presented. It is assumed that traffic flow at the entry and exit of that stretch is known. The design is built upon on a conservation of vehicles model and a velocity-density relationship given by some of the so called "fundamental diagrams." A nonlinear observer is designed that exploits the model structure to set a matrix of observer gains. Together with the design of the observer, it is convenient to estimate some traffic mixing factors that arise during the spatial discretization of the conservation of vehicles model and whose value indicates the traffic regimen: free or congested.

The paper first describes the traffic flow model and the density-velocity relationships used. After that, the design of the adaptive observer is undetaken and its convergence properties are analyzed. Simulation results and concluding remarks are then presented.

II. Traffic flow modeling

Traffic flow modeling is based on a conservation of vehicles principle that can be stated as

$$\frac{\partial \mathbf{N}(x,t)}{\partial t} = -\frac{\partial}{\partial x}\left\{\mathbf{V}(x,t)\mathbf{N}(x,t)\right\} \qquad (1)$$

where x is the longitudinal position along the freeway, t is the time, $\mathbf{N}(x,t)$ is the vehicle density at position x and time t and $\mathbf{V}(x,t)$ the longitudinal velocity. Both quantities $\mathbf{N}(x,t)$ and $\mathbf{V}(x,t)$ are aggregated for all the freeway lanes.

The model in Eq. (1) can be discretized in a set of sections of finite lenght, if the equation is integrated with respect to x in both sides. For this integration, upstream or downstream boundary conditions should be considered, depending on the traffic regimen being free or congested, as will be explained later on. Fig. 1 shows a schematic diagram of a four section freeway where the integration has been performed using upstream boundary conditions. The corresponding model has the form

Luis Alvarez-Icaza (alvar@pumas.iingen.unam.mx) is professor at the Instituto de Ingeniería, Universidad Nacional Autónoma de México, 04510, Coyoacán DF, México. Corresponding author.
Laura Munoz (lmunoz@me.berkeley.edu) and Xiotian Sun (sunx@me.berkeley.edu) are graduate students and Roberto Horowitz (horowitz@me.berkeley.edu) is professor at the Department of Mechanical Engineering, University of California at Berkeley, Berkeley, CA 94720, USA.

0-7803-8335-4/04/$17.00 ©2004 AACC

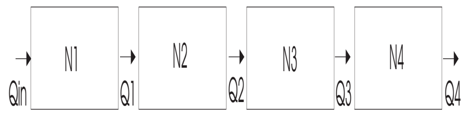

Fig. 1. Discrete section freeway model

$$\dot{n}_1 = \frac{1}{L_1}(q_{in} - q_1) \tag{2a}$$
$$\dot{n}_2 = \frac{1}{L_2}(q_1 - q_2) \tag{2b}$$
$$\dot{n}_3 = \frac{1}{L_3}(q_2 - q_3) \tag{2c}$$
$$\dot{n}_4 = \frac{1}{L_4}(q_3 - q_4) \tag{2d}$$

where n_i is the average vehicle density in section i, L_i the lenght of section i, q_i the flow between sections i and $i+1$, and q_{in} the inflow to the first section. Concatenation of models as the one in Eq. (2) makes it possible to model more complex freeway networks.

The flow q_i in the model of Eq. (2) can be expressed as

$$q_i = n_{q_i} v_{q_i} \tag{3}$$

where n_{q_i} and v_{q_i} are the density and velocity in the point where sections i and $i+1$ connect. Although for a general case of a hydrodynamic system, velocity and density are independent variables, for transportation systems there is abundant literature about the way drivers adjust their velocity depending on the density they percieve locally. This velocity-density relationship is stated through what is known as "fundamental diagrams." Fig. 2 shows two curves that correspond to two different fundamental diagrams. Two parts can be distinguished in the curves. In the first part, that corresponds to low densities, velocity is constant and characterizes free flow traffic where drivers travel at the maximum allowable speed. The second part of the curve, for higher densities, shows a decreasing value of velocity with the increase of density and occurs when the traffic is congested. In the first example shown in Fig. 2, velocity decreases linearly with density, when this exceeds a critical value[1], until getting to the point of traffic jam, where velocity is zero. In the second example, a driver reduces its velocity as a function of the square of the distance between him/hem and the driver in front. This distance is inversely proportional to density: more density implies less distance between vehicles and therefore smaller velocities.

In Eq. (2), n_i is used to model the average density in section i, while density n_{q_i} in the point connecting

[1]0.05 [veh/m] for the example in Fig. 2.

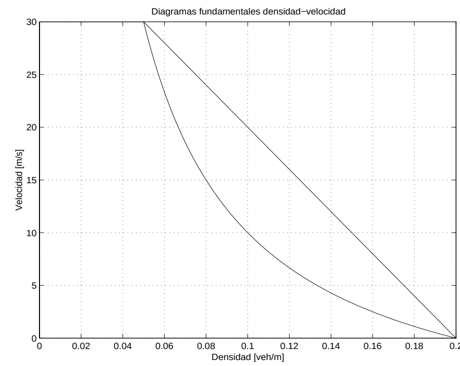

Fig. 2. Examples of fundamental diagrams

section i and $i+1$, was used in Eq. (3). It is therefore necessary to express n_{q_i} as a function of n_i, and for that purpose it is proposed to model flow q_i according to

$$q_1 = (\alpha_1 n_1 + (1-\alpha_1) n_2) v_{q_1} \tag{4a}$$
$$q_2 = (\alpha_2 n_2 + (1-\alpha_2) n_3) v_{q_2} \tag{4b}$$
$$q_3 = (\alpha_3 n_3 + (1-\alpha_3) n_4) v_{q_3} \tag{4c}$$
$$q_4 = n_4 v_{q_4} \tag{4d}$$

where $\alpha_i \in [0,1]$ are mixing factors related with the length of sections i and $i+1$ and the traffic condition: free or congested [6]. In this paper these factors are assumed unknown and constant for each traffic condition.

The terms in parenthesis in the right side of Eq. (4) imply that density n_{q_i} is a convex mixing of the average densities n_i in the neighbor sections. Velocity v_{q_i} is either known or can be calculated from a fundamental diagram and the values of n_i and α_i.

If Eqs. (2) and (4) are arranged in matrix form, they become

$$\dot{N} = L_{in} V_q A_\alpha N + B q_{in} \tag{5}$$

where

$$N = \begin{pmatrix} n_1 \\ n_2 \\ n_3 \\ n_4 \end{pmatrix}, \; L_{in} = \begin{pmatrix} 1/L_1 & 0 & 0 & 0 \\ 0 & 1/L_2 & 0 & 0 \\ 0 & 0 & 1/L_3 & 0 \\ 0 & 0 & 0 & 1/L_4 \end{pmatrix},$$

$$V_q = \begin{pmatrix} v_{q_1} & 0 & 0 & 0 \\ -v_{q_1} & v_{q_2} & 0 & 0 \\ 0 & -v_{q_2} & v_{q_3} & 0 \\ 0 & 0 & -v_{q_3} & v_{q_4} \end{pmatrix}, B = \begin{pmatrix} 1/L_1 \\ 0 \\ 0 \\ 0 \end{pmatrix}$$

$$A_\alpha = \begin{pmatrix} -\alpha_1 & -(1-\alpha_1) & 0 & 0 \\ 0 & -\alpha_2 & -(1-\alpha_2) & 0 \\ 0 & 0 & -\alpha_3 & -(1-\alpha_3) \\ 0 & 0 & 0 & -1 \end{pmatrix}$$

Now assume that the input flow q_{in} is constant. The stability of the equilibria $\tilde{q}_i = q_i - q_{in}$ will be investigated. It is important to remark that the constant value $q_i = q_{in}$ can be obtained with two combinations of density and velocity: one in the free flow region and other in the congested flow region, respectively. Define the following Lyapunov function candidate

$$W_1 = \begin{pmatrix}\tilde{q}_1 & \tilde{q}_2 & \tilde{q}_3 & \tilde{q}_4\end{pmatrix} \begin{pmatrix} L_1 & 0 & 0 & 0 \\ 0 & L_2 & 0 & 0 \\ 0 & 0 & L_3 & 0 \\ 0 & 0 & 0 & L_4 \end{pmatrix} \begin{pmatrix}\tilde{q}_1 \\ \tilde{q}_2 \\ \tilde{q}_3 \\ \tilde{q}_4\end{pmatrix} \quad (6)$$

Taking the time derivative of Eq. (6), and assuming for simplicity that $L_i = L \, \forall i$, it can be shown that

$$\dot{W}_1 = \begin{pmatrix}\tilde{q}_1 & \tilde{q}_2 & \tilde{q}_3 & \tilde{q}_4\end{pmatrix} \begin{pmatrix} \frac{\partial \tilde{q}_1}{\partial n_{q_1}} & 0 & 0 & 0 \\ 0 & \frac{\partial \tilde{q}_2}{\partial n_{q_2}} & 0 & 0 \\ 0 & 0 & \frac{\partial \tilde{q}_3}{\partial n_{q_3}} & 0 \\ 0 & 0 & 0 & \frac{\partial \tilde{q}_4}{\partial n_{q_4}} \end{pmatrix}$$
$$\begin{pmatrix} 1-2\alpha_1 & -(1-\alpha_1) & 0 & 0 \\ \alpha_2 & 1-2\alpha_2 & -(1-\alpha_2) & 0 \\ 0 & \alpha_3 & 1-2\alpha_3 & -1(-\alpha_3) \\ 0 & 0 & 1 & -1 \end{pmatrix} \begin{pmatrix}\tilde{q}_1 \\ \tilde{q}_2 \\ \tilde{q}_3 \\ \tilde{q}_4\end{pmatrix} \quad (7)$$

Sufficient conditions for all the eigenvalues of the matrix in the quadratic form in Eq. (7) to be negative, and therefore for the equilibria $\tilde{q}_i = 0$ to be asymptotically stable, are that *i)* $0.5 < \alpha_i < 1$ and *ii)* $\frac{\partial \tilde{q}_i}{\partial n_{q_i}} > 0$. The second condition implies free flow traffic, as only in this case the derivative is positive. The other equilibria, in the congested traffic region, is unstable for this upstream boundary condition.

It is possible to develop a similar model to the one in Eq. (5) if the boundary conditions are taken at the exit of the freeway stretch. The most important difference between both cases is that now the congested point in the diagram is asymptotically stable if $0 < \alpha_i < 0.5$. These results are consistent with those presented in [7], although the modeling paradigm used for the flows q_i in this paper is different to that in [7].

III. Density estimation

Once the dynamic model for the freeway stretch is established, an observer for the density is proposed. For this purpose, it is assumed that there are sensors of flow and velocity at the beginning of the stretch, between sections 1 and 2, 3 and 4, and at the end of the stretch. Typical sensors for flow and velocity are represented in Fig. 3. They are composed of two coils placed on the asphalt. Coils are phased out a given distance in the direction of the traffic. Vehicle presence changes the magnetic properties of the coils and induces pulses. Because the distance between coils is known, time between pulses gives vehicle velocity. Number of pulses per unit time gives the flow. Therefore, the following quantities are assumed to be known: q_{in}, q_1, q_3, q_4, v_{q_1}, v_{q_3} and v_{q_4}.

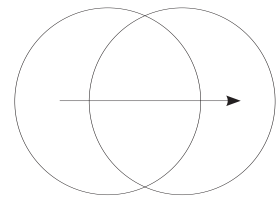

Fig. 3. Flow and velocity sensors

The following observer for vehicle density is proposed

$$\dot{\hat{N}} = L_{in} \hat{V}_q \hat{A}_\alpha \hat{N} + B q_{in} + K(y - \hat{y}) \quad (8)$$

where $\hat{N}$ is the estimated densities vector, $\hat{A}_\alpha$ is matrix built with the estimated α_i,

$$\hat{V}_q = \begin{pmatrix} v_{q_1} & 0 & 0 & 0 \\ -v_{q_1} & \hat{v}_{q_2} & 0 & 0 \\ 0 & -\hat{v}_{q_2} & v_{q_3} & 0 \\ 0 & 0 & -v_{q_3} & v_{q_4} \end{pmatrix},$$

$$y = \begin{pmatrix} q_1 \\ q_3 \\ q_4 \end{pmatrix}, \; \hat{y} = \begin{pmatrix} \hat{q}_1 \\ \hat{q}_3 \\ \hat{q}_4 \end{pmatrix}$$

and K is a gain matrix to be defined below.

It is possible to express y and $\hat{y}$ as

$$y = V_{q_s} A_{\alpha_s} N; \quad \hat{y} = V_{q_s} \hat{A}_{\alpha_s} \hat{N}$$

with $V_{q_s} = diag\{v_{q_1}, v_{q_3}, v_{q_4}\}$,

$$A_{\alpha_s} = \begin{pmatrix} \alpha_1 & (1-\alpha_1) & 0 & 0 \\ 0 & 0 & \alpha_3 & (1-\alpha_3) \\ 0 & 0 & 0 & 1 \end{pmatrix}$$

and $\hat{A}_{\alpha_s}$ uses the estimated α_i. If the density estimation error vector is defined by $\tilde{N} = N - \hat{N}$ and Eqs. (5) and (8) are used, the dynamics for the density estimation error is

$$\begin{aligned} \dot{\tilde{N}} = & L_{in} V_q A_\alpha \tilde{N} + L_{in} \tilde{V}_q \hat{A}_\alpha \hat{N} + L_{in} V_q \tilde{A}_\alpha \hat{N} \\ & - K V_{q_s} A_{\alpha_s} \tilde{N} - K V_{q_s} \tilde{A}_{\alpha_s} \hat{N} \end{aligned} \quad (9)$$

where

$$\tilde{V}_q = \begin{pmatrix} 0 & 0 & 0 & 0 \\ 0 & \tilde{v}_{q_2} & 0 & 0 \\ 0 & -\tilde{v}_{q_2} & 0 & 0 \\ 0 & 0 & 0 & 0 \end{pmatrix},$$

$$\tilde{A}_\alpha = \begin{pmatrix} -\tilde{\alpha}_1 & \tilde{\alpha}_1 & 0 & 0 \\ 0 & -\tilde{\alpha}_2 & \tilde{\alpha}_2 & 0 \\ 0 & 0 & -\tilde{\alpha}_3 & \tilde{\alpha}_3 \\ 0 & 0 & 0 & 0 \end{pmatrix}$$

$$\tilde{A}_{\alpha_s} = \begin{pmatrix} \tilde{\alpha}_1 & -\tilde{\alpha}_1 & 0 & 0 \\ 0 & 0 & \tilde{\alpha}_3 & -\tilde{\alpha}_3 \\ 0 & 0 & 0 & 0 \end{pmatrix}$$

The parameter estimation error is defined as $\tilde{\theta} = \theta - \hat{\theta} = (\alpha_1, \alpha_2, \alpha_3)^T - (\hat{\alpha}_1, \hat{\alpha}_2, \hat{\alpha}_3)^T$ and the following Lyapunov function candidate is introduced

$$W = \tilde{N}^T \tilde{N} + \frac{1}{2} \tilde{\theta}^T \Gamma^1 \tilde{\theta} \quad (10)$$

to analyze the stability of the equilibrium $\tilde{N} = 0, \tilde{\theta} = 0$. Deriving W with respect to time leads to

$$\begin{aligned} \dot{W} &= \tilde{N}^T \left(L_{in} V_q A_\alpha + A_\alpha^T V_q^T L_{in} \right) \tilde{N} \\ &- \tilde{N}^T \left(K V_{q_s} A_{\alpha_s} + A_{\alpha_s}^T V_{q_s} K^T \right) \tilde{N} \\ &+ \tilde{N}^T L_{in} \tilde{V}_q \hat{A}_\alpha \hat{N} + \hat{N}^T \hat{A}_\alpha^T \tilde{V}_q^T L_{in} \tilde{N} \\ &+ \tilde{N}^T \left(L_{in} V_q \tilde{A}_\alpha - K V_{q_s} \tilde{A}_{\alpha_s} \right) \hat{N} \\ &+ \hat{N}^T \left(\tilde{A}_\alpha^T V_q^T L_{in} - \tilde{A}_{\alpha_s}^T V_{q_s}^T K^T \right) \tilde{N} + \dot{\tilde{\theta}}^T \Gamma^{-1} \tilde{\theta} \end{aligned} \quad (11)$$

The third term in the right hand side can be expressed as

$$\tilde{N}^T L_{in} \tilde{V}_q \hat{A}_\alpha \hat{N} = \tilde{N}^T F G \tilde{N}$$

where

$$F = \begin{pmatrix} 0 & 0 & 0 & 0 \\ 0 & 1/L_2 & 0 & 0 \\ 0 & -1/L_3 & 0 & 0 \\ 0 & 0 & 0 & 0 \end{pmatrix}, \; G = \begin{pmatrix} 0 & 0 & 0 & 0 \\ 0 & \gamma_2 & \gamma_3 & 0 \\ 0 & 0 & 0 & 0 \\ 0 & 0 & 0 & 0 \end{pmatrix}$$

and $\gamma_2, \gamma_3 \geq 0$. These result is derived using a fundamental diagrams, where it is noted that the velocity is different form zero for density values between zero and jam density. As the fundamental diagrams are not growing functions it is always the case that

$$v(n_1) - v(n_2) = -\gamma(n_1 - n_2) \; ; \gamma \geq 0 \quad (12)$$

therefore $\tilde{v}_{q_2} = -\gamma_2 \tilde{n}_2 - \gamma_3 \tilde{n}_3$. In particular, it should be noticed that γ_i value depends on $\max_n |\partial v(n)/\partial n|$ and the maximum values of v_{q_i} and $\hat{n}_i$.

In addition, matrix

$$L_{in} V_q A_\alpha + A_\alpha^T V_q^T L_{in} \preceq 0 \quad (13)$$

if $0.5 < \alpha_i \preceq 1$. Therefore, if matrix K is chosen according to

$$\left(K V_{q_s} A_{\alpha_s} - F G \right) + \left(A_{\alpha_s}^T V_{q_s} K^T - G^T F^T \right) \geq 0 \quad (14)$$

the first four terms of Eq. (11) become negative semidefinite. The other terms can be rewritten as

$$\begin{aligned} & 2\tilde{N}^T \left(L_{in} V_q \tilde{A}_\alpha - K V_{q_s} \tilde{A}_{\alpha_s} \hat{N} \right) + \dot{\tilde{\theta}}^T \Gamma^{-1} \tilde{\theta} = \\ & 2\tilde{N}^T \left(L_{in} \Psi_3(N, \hat{N}) - K \Psi_4(\hat{N}) \right) \tilde{\theta} + \dot{\tilde{\theta}}^T \Gamma^{-1} \tilde{\theta} \end{aligned} \quad (15)$$

where

$$\Psi_3 = \begin{pmatrix} -v_{q_1}(\hat{n}_1 - \hat{n}_2) & 0 & 0 \\ v_{q_1}(\hat{n}_1 - \hat{n}_2) & -v_{q_2}(\hat{n}_3 - \hat{n}_3) & 0 \\ 0 & v_{q_2}(\hat{n}_2 - \hat{n}_3) & -v_{q_3}(\hat{n}_3 - \hat{n}_3) \\ 0 & 0 & v_{q_3}(\hat{n}_3 - \hat{n}_4) \end{pmatrix}$$

$$\Psi_4 = \begin{pmatrix} v_{q_1}(\hat{n}_1 - \hat{n}_2) & 0 & 0 \\ 0 & 0 & v_{q_3}(\hat{n}_3 - \hat{n}_4) \\ 0 & 0 & 0 \end{pmatrix}$$

If a gradient adaptation law is chosen

$$\dot{\theta} = \Gamma \Psi_4^T \tilde{y} \; , \quad (16)$$

the time derivative of W can be rewritten in matrix for as

$$\dot{W} = -(\tilde{\theta} \quad \tilde{N}) \begin{pmatrix} 2\Psi_4^T & -2\Psi_4^T A_{\alpha_s} V_{q_s} \\ -2(K\Psi_4 - L_{in}\Psi_3) & H \end{pmatrix} \begin{pmatrix} \tilde{\theta} \\ \tilde{N} \end{pmatrix} \quad (17)$$

where

$$\begin{aligned} H = &- \left(L_{in} V_q A_\alpha + A_\alpha^T V_q^T L_{in} \right) - \left(K V_{q_s} A_{\alpha_s} - F G \right) \\ &- \left(A_{\alpha_s}^T V_{q_s} K^T - G^T F^T \right) \end{aligned}$$

The matrix in a quadratic form in Eq. (17) is an S-matriz [8], therefore there exists scaling factors on each of the states and estimates such that $\dot{W} \preceq 0$. From this, stability of $\tilde{N}$ and $\tilde{\theta}$ follows. If, in addition, Barbalat's Lemma is used [8], it can be shown that $\lim_{t\to\infty} q_i - \hat{q}_i = 0$. To get $\lim_{t\to\infty} \tilde{\theta} = 0$ persistence of excitation is needed.

The stability analysis for the congested case, when the boundary conditions are fixed downstream is realized in a similar fashion and is not presented in this paper for economy of space. It is only important to mention that mixing factors must satisfy in this case $0 < \alpha_i < 0.5$.

IV. Simulation results

This section presents the results of two simulations that illustrate the observer functioning. One simulation is for free flow traffic and the other for congested traffic. Conditions for simulations are set as follows. Four freeway sections, as shown in Fig. 1, each one of them with a length of 500 $[m]$, were simulated during one and a half hour. For the free flow case, mixing factor are $\alpha_i = 0.6; i = 1, 2, 3$ and the input flow was $q_{in} = 1.0$ $[veh/s]$. For the congested case, the mixing factors are $\alpha_i = 0.4; i = 1, 2, 3$ and the output flow was $q_{out} = 1.3$ $[veh/s]$. In both cases, the simulation used the fundamental diagram that is shown as an hyperbola if Fig. 2, in which the velocity is inversely proportional to the local density. Free flow velocity is 30 $[m/s]$, critical density is 0.05 $[veh/m]$ and jam density is 0.2 $[veh/m]$. Initial densities were set around $0.05[veh/m]$ and the initial estimates differ between 20-25% from the real ones. Matrix K for the free flow case is

$$K = 1/500 \begin{pmatrix} 0.31 & 0 & 0 \\ 0.31 & 0.31 & 0 \\ 0 & 0.31 & 0.31 \\ 0 & 0 & 0.31 \end{pmatrix},$$

and for the congested case a similar matrix was used.

Figs. 4-7 show the flow between sections and the estimation errors for density, flow and mixing factors for the case of free flow. Figs. 8-11 show the same results for the congested case.

It is important to note the relative fast convergence of the density estimation for both cases: free flow and congested traffic. Mixing factor estimation errors do not converge to zero, as it can be expected, because the excitation signal are relatively poor in both cases. However these error have no effect on the estimation errors of the flow and density.

V. Conclusions

An algorithm to estimate vehicle density in situations where the sensor is not in the location needed for on-ramp metering control or is faulty was described. The scheme was based on a conservation of vehicles model and assumed the existence of a fundamental diagram describing the velocity-density relationship. From this, and adaptive observer is proposed whose stable behavior depends on the selection of a gain matrix according with traffic condition: free or congested. The scheme was proved with simulations that confirm analytical findings. It is still necessary to apply the scheme to more complex scenarios and combined it with on-ramp metering control algorithms.

References

[1] P. Varaiya, "Smart cars on smart roads: problems of control," IEEE Transactions on Automatic Control, vol. AC-38, no. 2, pp. 195–207, 1993.

[2] R. Horowitz and P. Varaiya, "Control design of an automated highway system," Proceedings of the IEEE, vol. 88, pp. 913–925, 2000.

[3] M. Papageorgiou, J.-M. Blosseville, and H. Hadi-Salem, "Modelling and real-time control of traffic flow on the southern part of Boulevard Peripherique in Paris: Part i: Modelling and part ii: Coordinated on-ramp metering," Transportation Research A, vol. 24A, no. 5, pp. 345–370, 1990.

[4] M. Papageorgiou, H. Habib, and J. Blosseville, "ALINEA: a local feedback control law for on-ramp metering control," Transportation Research Record, vol. 1320, pp. 58–64, 1991.

[5] H. Zhang, S. Ritchie, and W. Recker, "Some general results on the optimal ramp control problem," Transportation Research Part C: Emerging Technologies, vol. 4, pp. 51–69, 1996.

[6] P. Li and A. Shrivastava, "Traffic flow stability induced by constant time headway policy for adaptive cruise control vehicles," Transportation Research Part C: Emerging Technologies, vol. 10, pp. 275–301, 2002.

[7] S. Swaminathan and P. Li, "Traffic flow stability induced by arbitrary adaptive cruise control policy," in Proceedings of the American Control Conference, 2003, pp. 4101–4106.

[8] H. K. Khalil, Nonlinear Systems, 2nd ed. USA: Prentice-Hall, 1996.

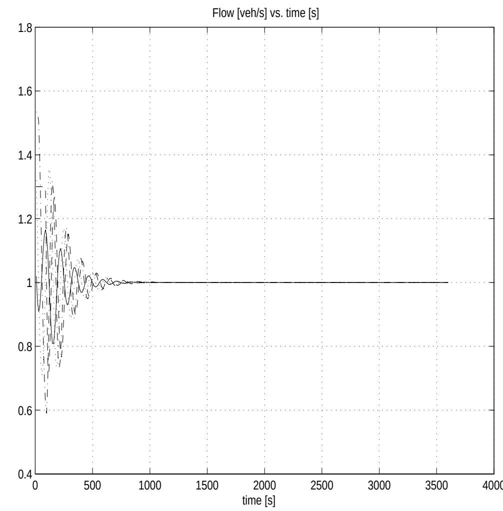

Fig. 4. Free flow: vehicle flow (section 1: solid, section 2: dots, section 3: dash-dot, section 4: dash)

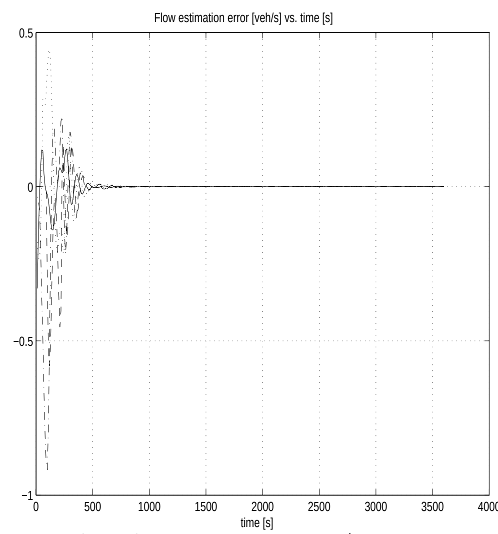

Fig. 5. Free flow: flow estimation error (section 1: solid, section 2: dots, section 3: dash-dot, section 4: dash)

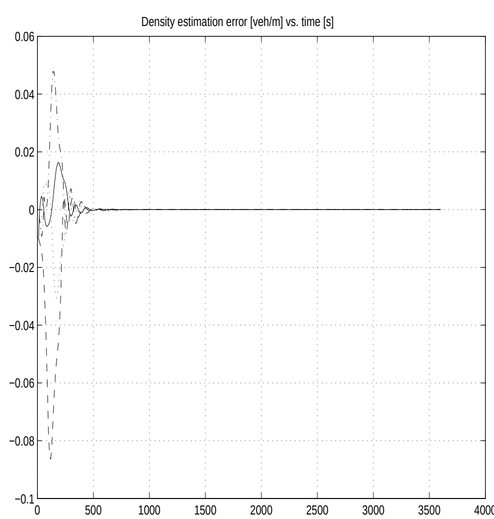

Fig. 6. Free flow: density estimation error (section 1: solid, section 2: dots, section 3: dash-dot, section 4: dash)

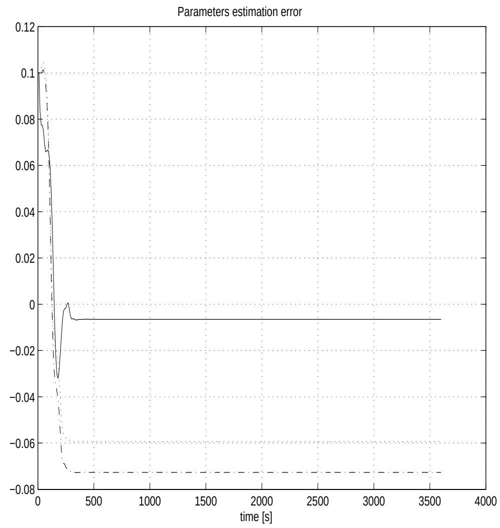

Fig. 7. Free flow: parameter estimation error (section 1: solid, section 2: dots, section 3: dash-dot, section 4: dash)

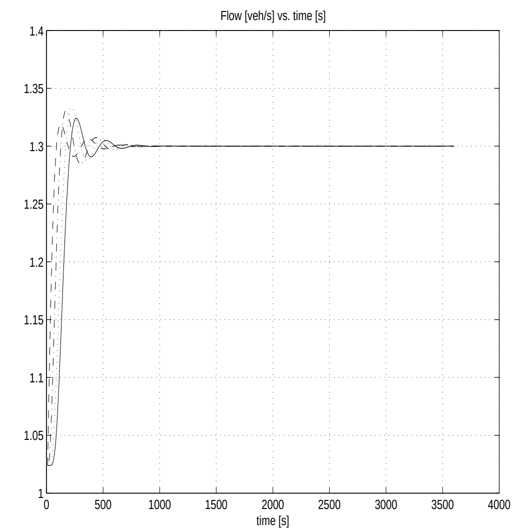

Fig. 8. Congested: vehicle flow (section 1: solid, section 2: dots, section 3: dash-dot, section 4: dash)

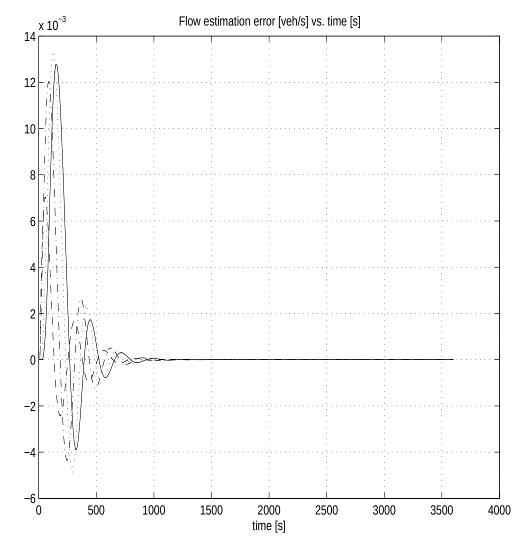

Fig. 9. Congested: flow estimation error (section 1: solid, section 2: dots, section 3: dash-dot, section 4: dash)

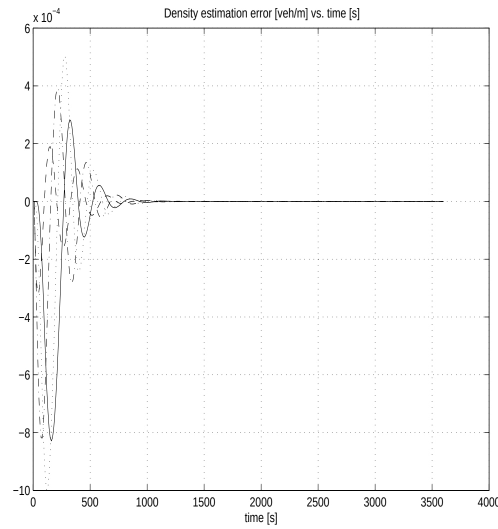

Fig. 10. Congested: density estimation error (section 1: solid, section 2: dots, section 3: dash-dot, section 4: dahs)

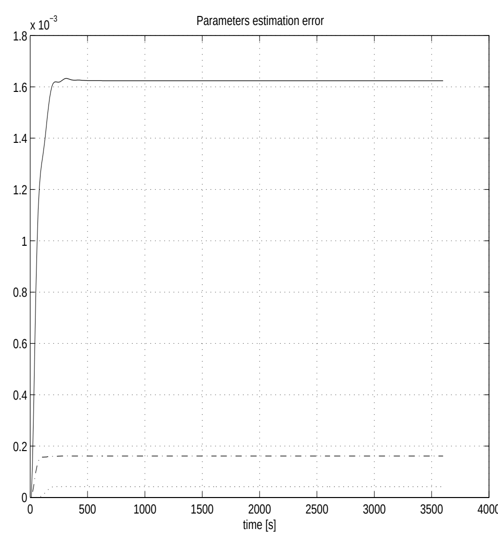

Fig. 11. Congested: parameter estimation error (section 1: solid, section 2: dots, section 3: dash-dot, section 4: dahs)